

Supporting Information

Materials design of edge-modified polymeric carbon nitride nanoribbons for photocatalytic CO₂ reduction reaction

Shaohua Liu,^a Yi Li,^{ab} Yongfan Zhang,^{*ab} Wei Lin^{*ab}

^a State Key Laboratory of Photocatalysis on Energy and Environment, College of Chemistry,
Fuzhou University, Fuzhou 350108, P.R. China

^b Fujian Provincial Key Laboratory of Theoretical and Computational Chemistry, Xiamen
University, Xiamen, Fujian 361005, China

E-mail: zhangyf@fzu.edu.cn (Y. Zhang); wlin@fzu.edu.cn (W. Lin)

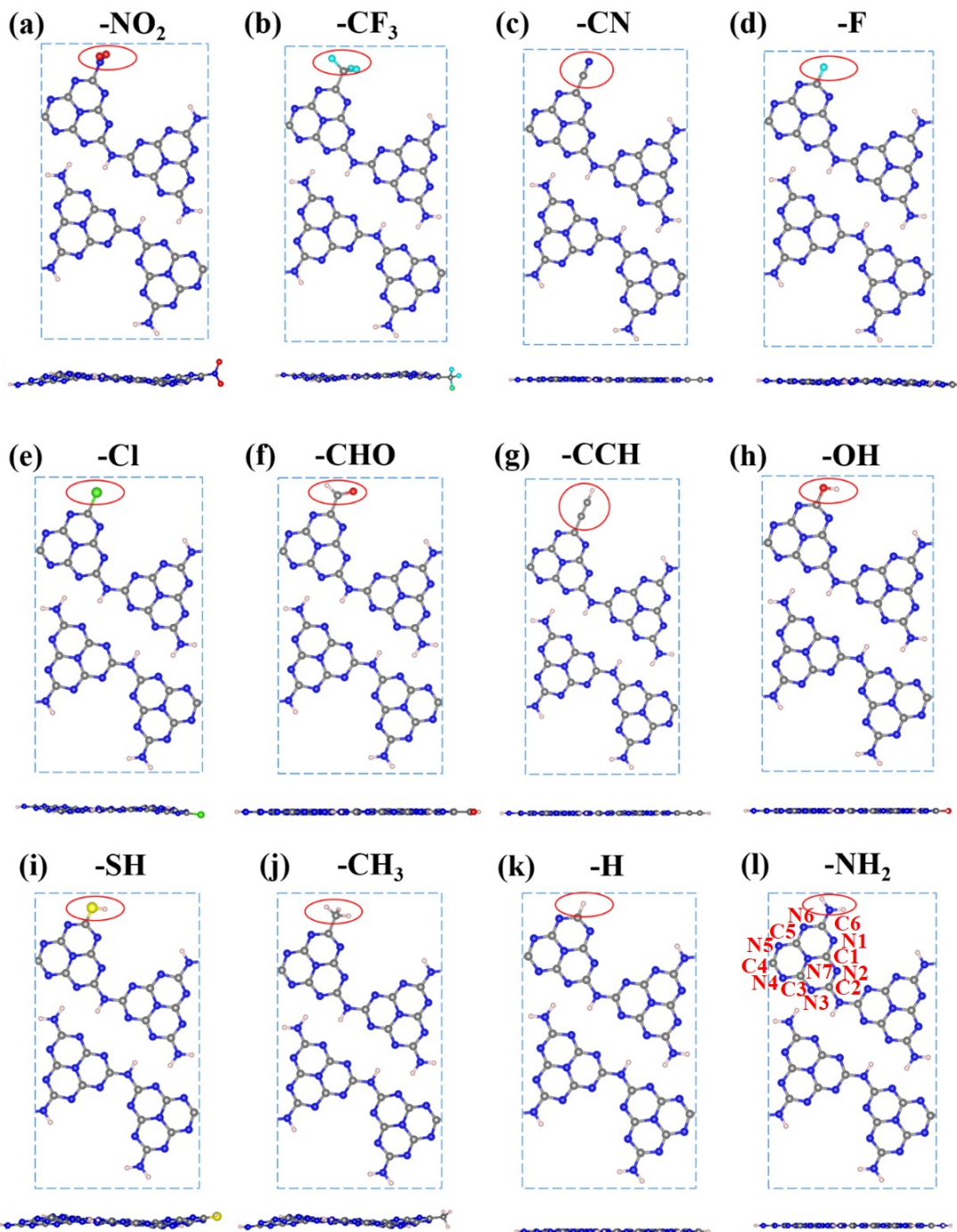


Fig. S1 Top and side views of edge-modified melon-based CN nanoribbons (X-MNRs, X = (a) -NO₂; (b) -CF₃; (c) -CN; (d) -CHO; (e) -F; (f) -Cl; (g) -C≡CH; (h) -OH; (i) -SH; (j) -CH₃; (k) -H; (l) -NH₂). Grey, brown, pink, red, yellow, blue, and green represent C, N, H, O, S, F, and Cl atoms, respectively.

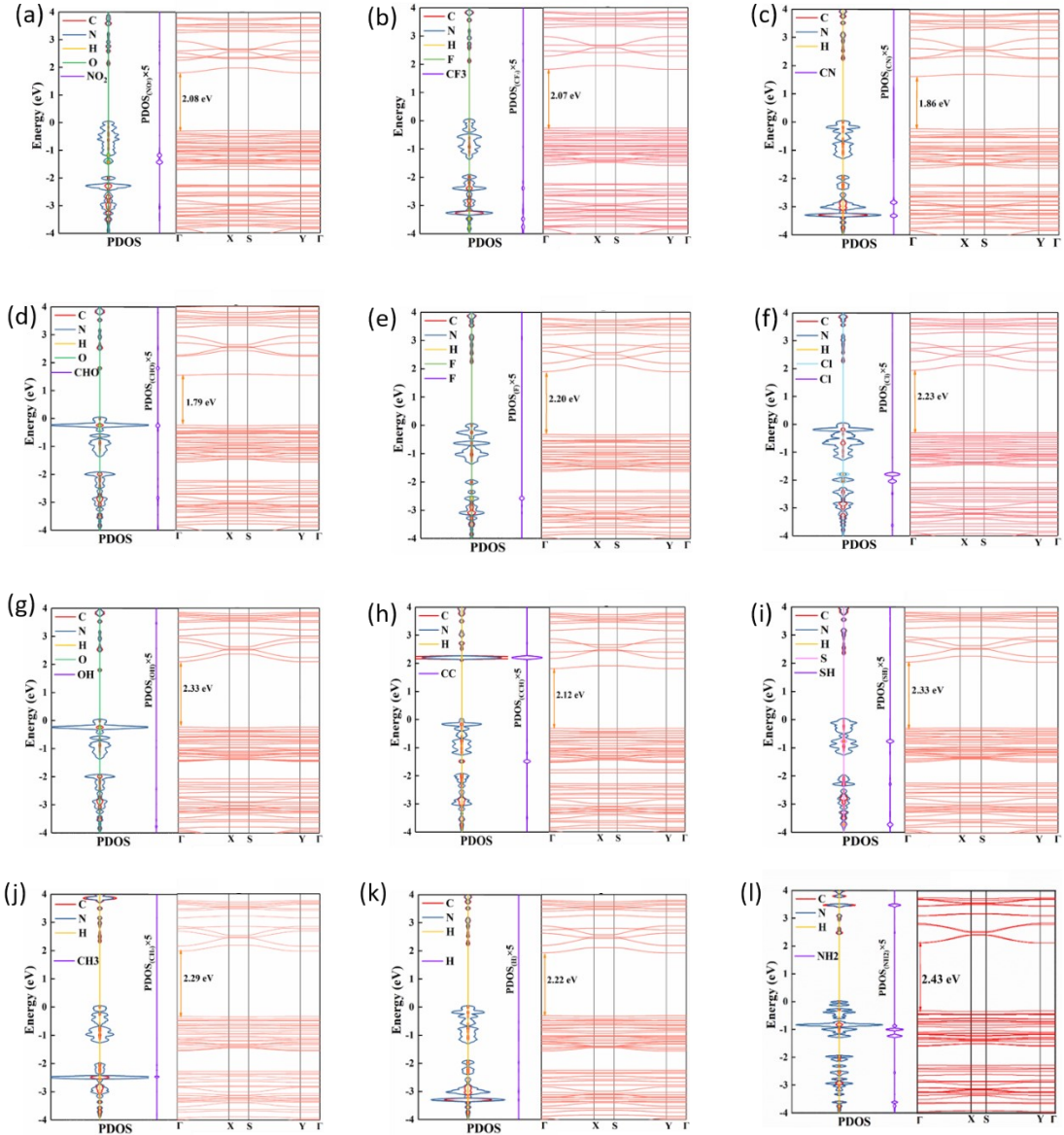


Fig. S2 The projected Density of states (pDOS) and band structures of edge-modified melon-based CN Nanoribbons (X-MNRs, X = (a) -NO₂; (b) -CF₃; (c) -CN; (d) -CHO; (e) -F; (f) -Cl; (g) -OH; (h) -C≡CH; (i) -SH; (j) -CH₃; (k) -H; (l) -NH₂)

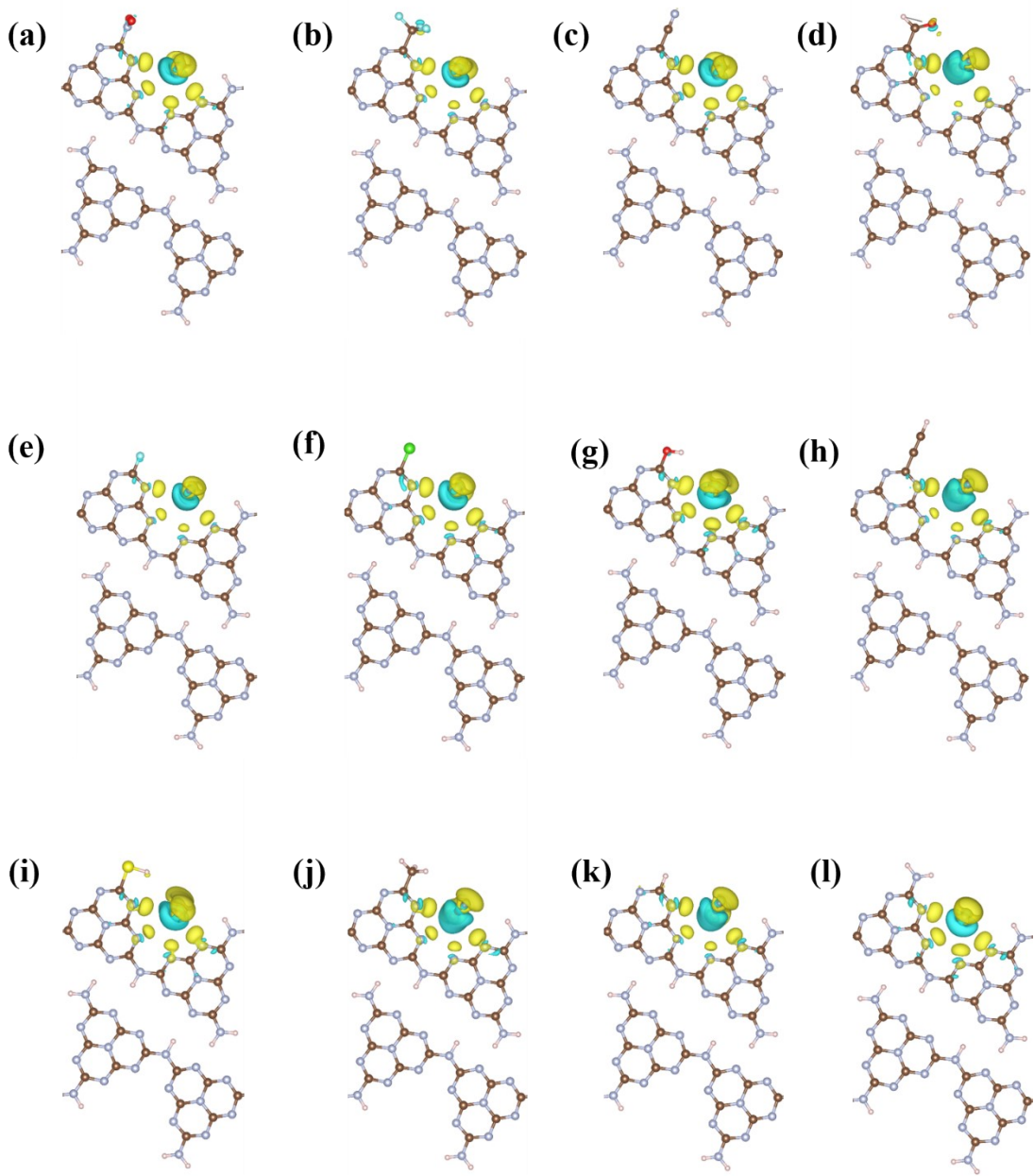


Fig. S3 Charge density difference of CO_2 adsorption on edge-modified melon-based CN nanoribbons (X-MNRs, X = (a) $-\text{NO}_2$; (b) $-\text{CF}_3$; (c) $-\text{CN}$; (d) $-\text{CHO}$; (e) $-\text{F}$; (f) $-\text{Cl}$; (g) $-\text{OH}$; (h) $-\text{C}\equiv\text{CH}$; (i) $-\text{SH}$; (j) $-\text{CH}_3$; (k) $-\text{H}$; (l) $-\text{NH}_2$). The yellow and green areas represent the positive and negative values of electrons, respectively. Grey, brown, pink, red, yellow, blue, and green balls represent C, N, H, O, S, F, and Cl atoms, respectively.

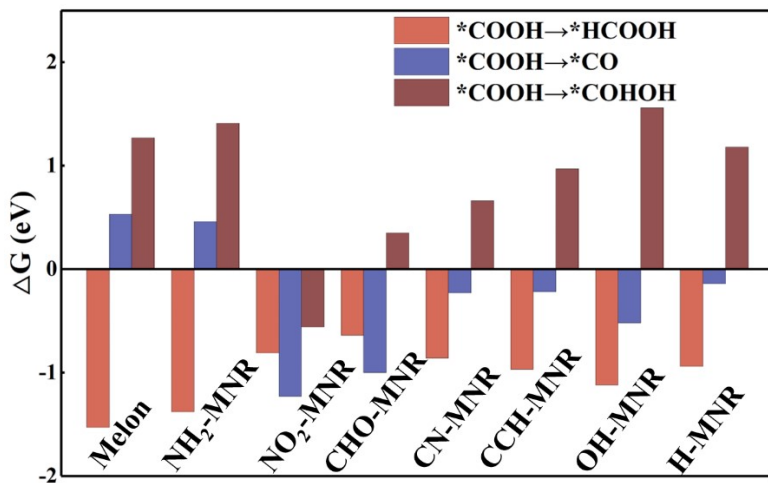


Fig. S4 The $^*\text{COOH}$ hydrogenation competitive elementary reaction of melon-based CN and edge-modified melon-based CN nanoribbons (X-MNRs, X = -NH₂, -NO₂, -CHO, -CN, -C≡CH, -OH, and -H).

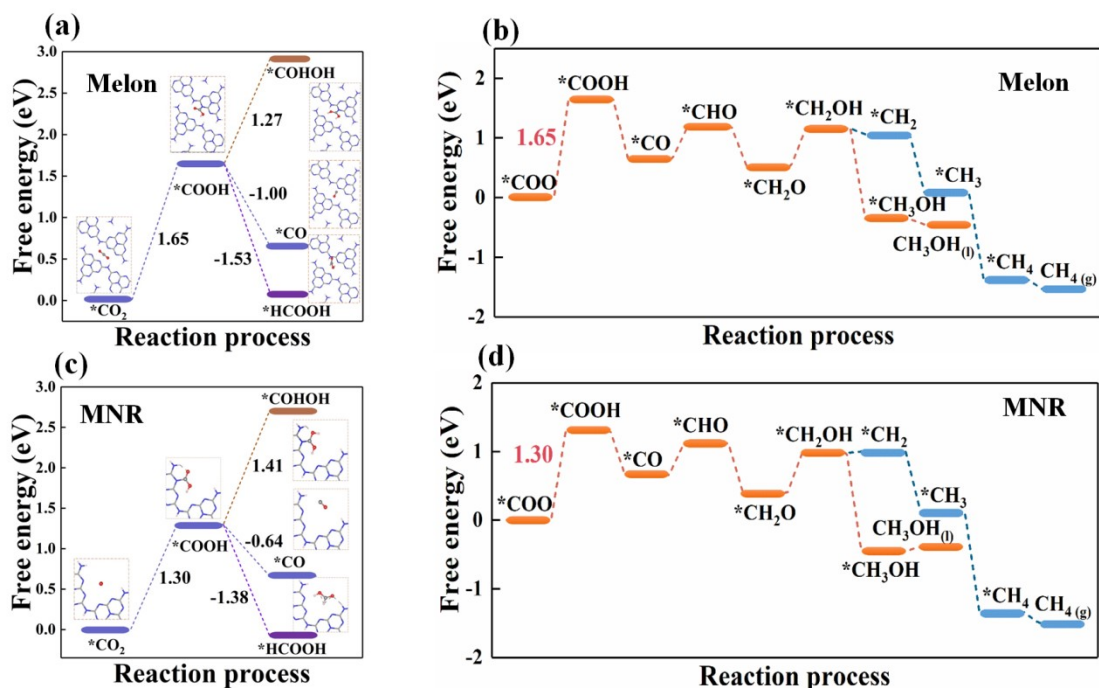


Fig. S5 (a) Two-electron and (b) six/eight-electron reaction process of CO₂ reduction by melon; (c) two-electron and (d) six/eight-electron reaction process of CO₂ reduction by MNR.

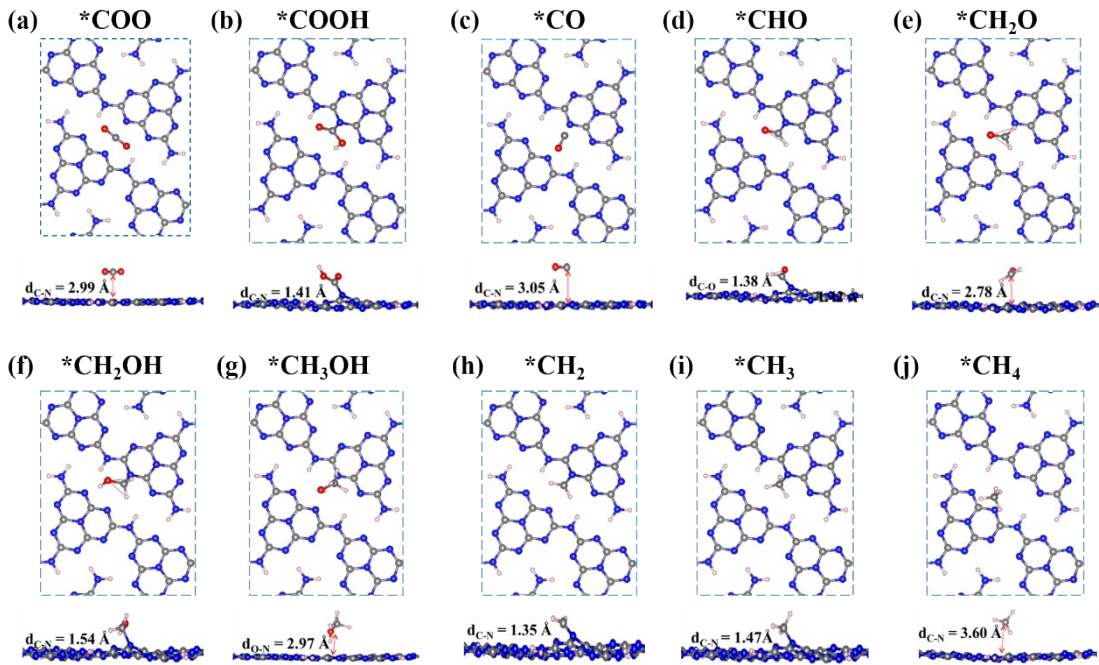


Fig. S6 Top and side views of the structure of the CO_2 reduction reaction intermediate of melon, where grey, blue, pink, and red represent C, N, H, and O atoms.

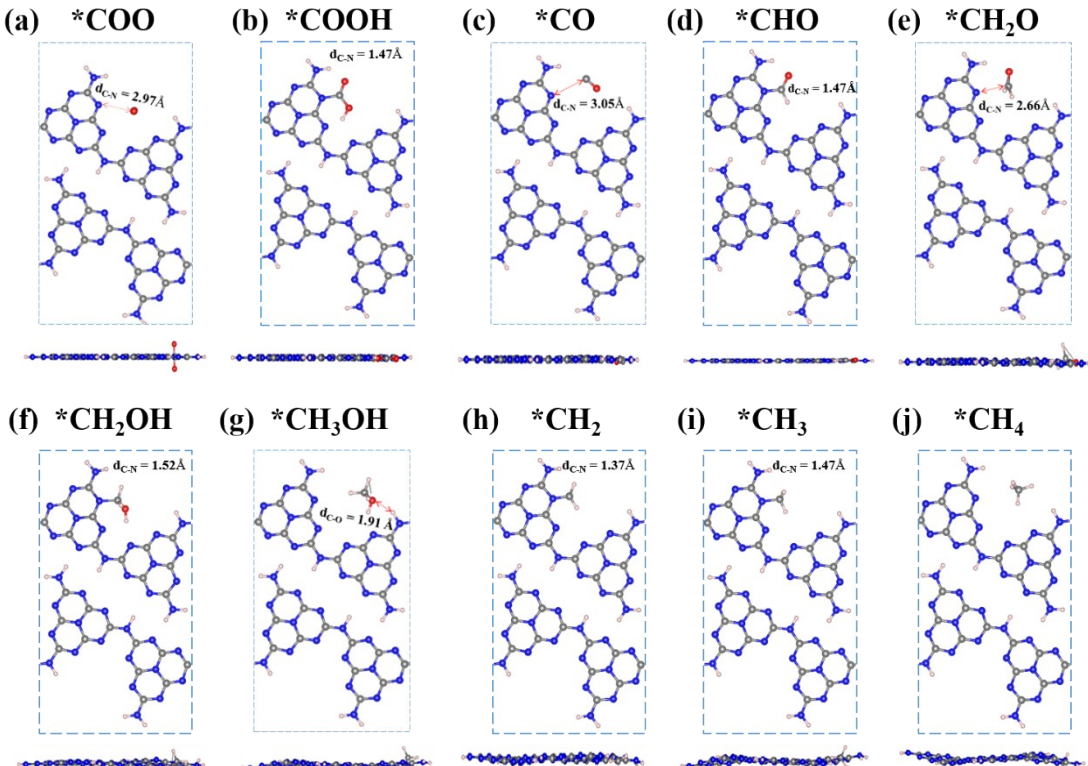


Fig. S7 Top and side views of the structure of the CO_2 reduction reaction intermediate of edge-modified melon-based CN nanoribbons ($\text{NH}_2\text{-MNR}$), where grey, blue, pink, and red represent C, N, H, and O atoms.

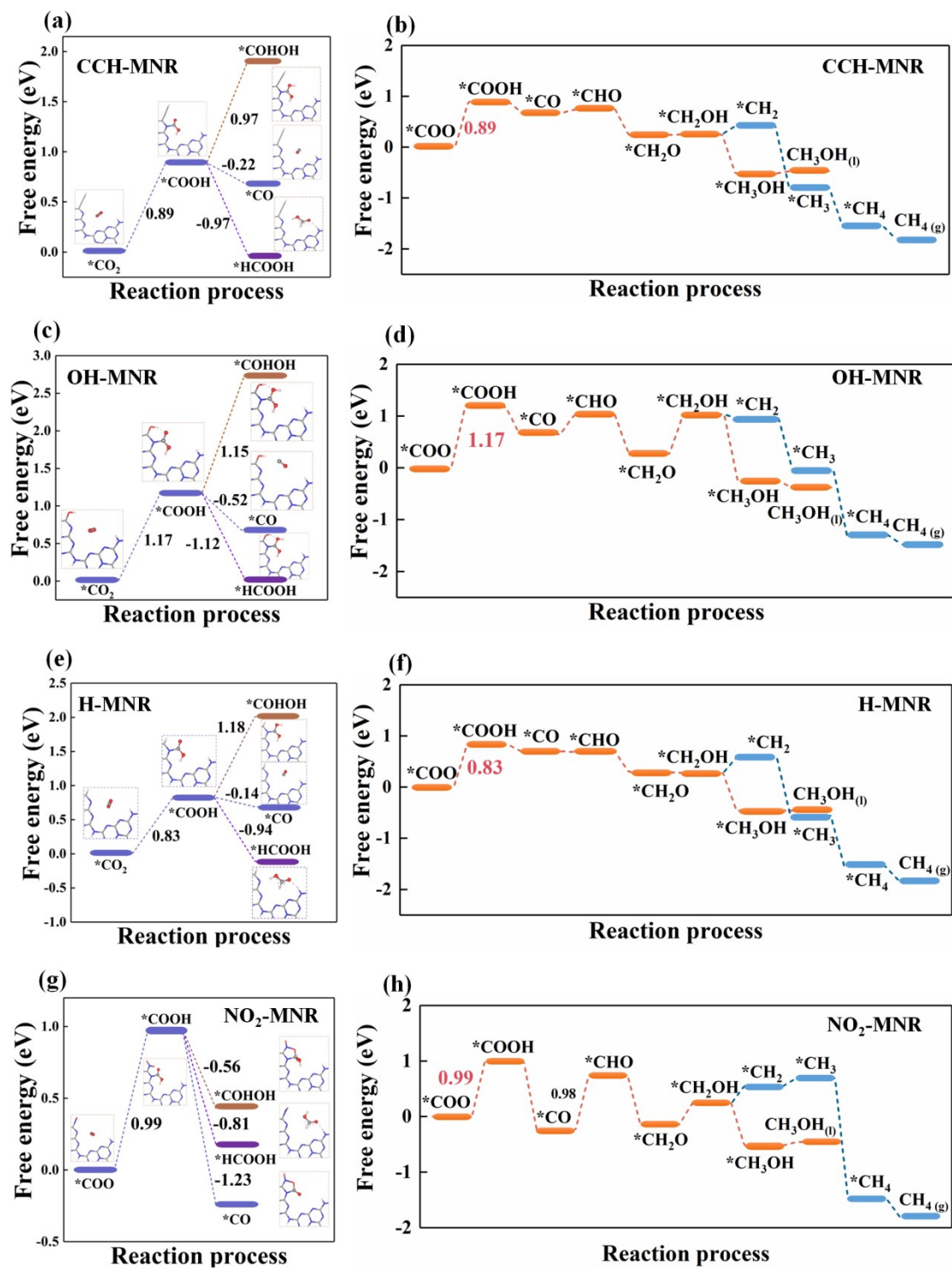


Fig. S8 Two-electron and six/eight-electron reaction process of CO₂ reduction by (a and b) CCH-MNR; (c and d) OH-MNR; (e and f) H-MNR; and (g and h) NO₂-MNR.

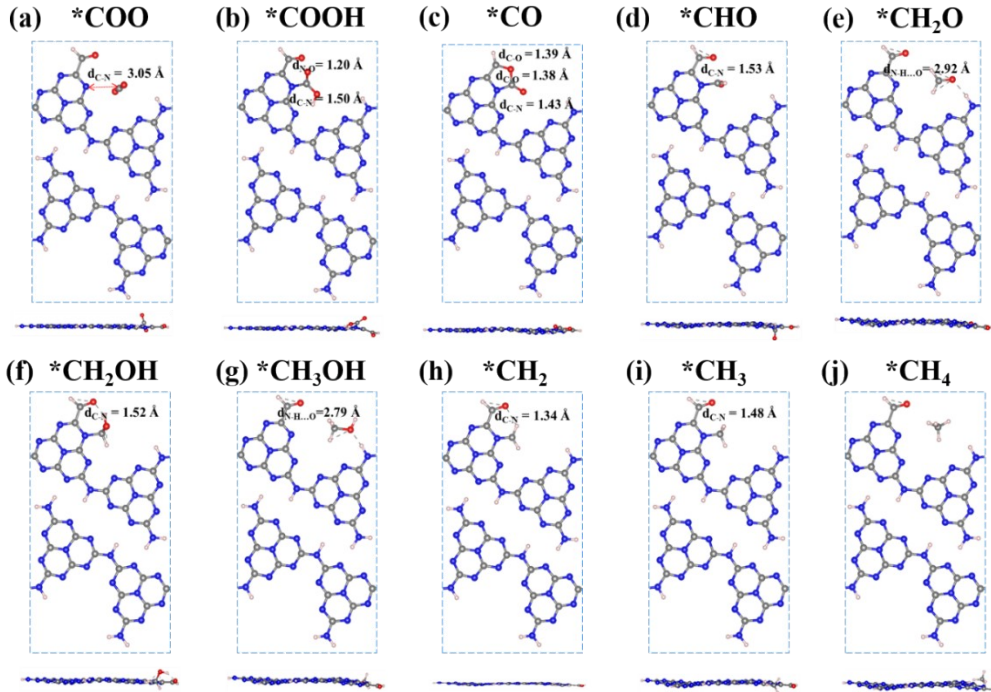


Fig.S9 Top and side views of the structure of the CO₂ reduction reaction intermediate of edge-modified melon-based CN nanoribbons (CHO-MNR), where grey, blue, pink, and red represent C, N, H, and O atoms.

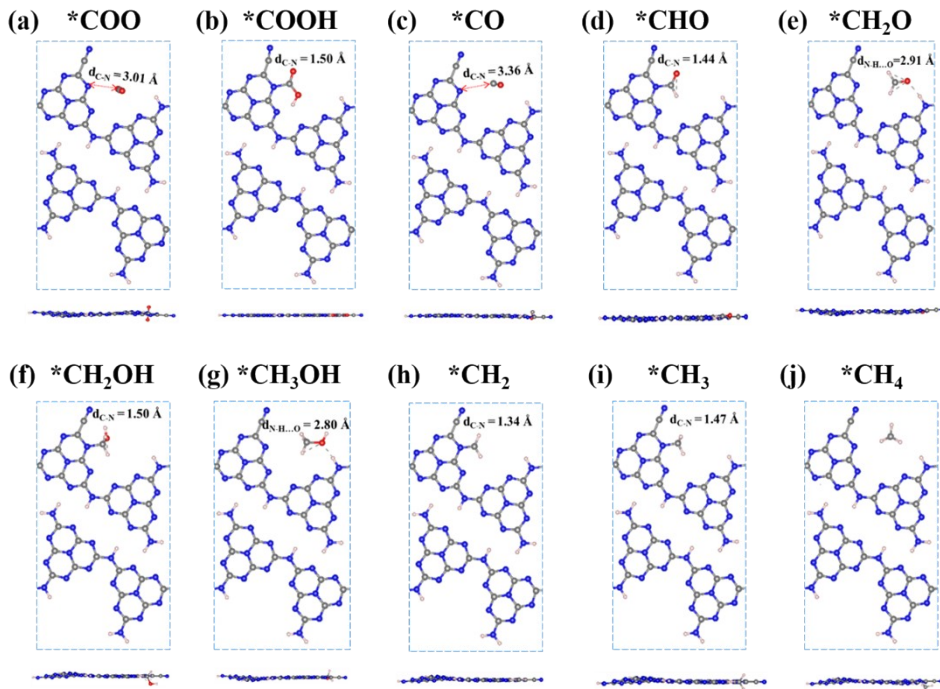


Fig. S10 Top and side views of the structure of the CO₂ reduction reaction intermediate of edge-modified melon-based CN nanoribbons (CN-MNR), where grey, blue, pink, and red represent C, N, H, and O atoms.

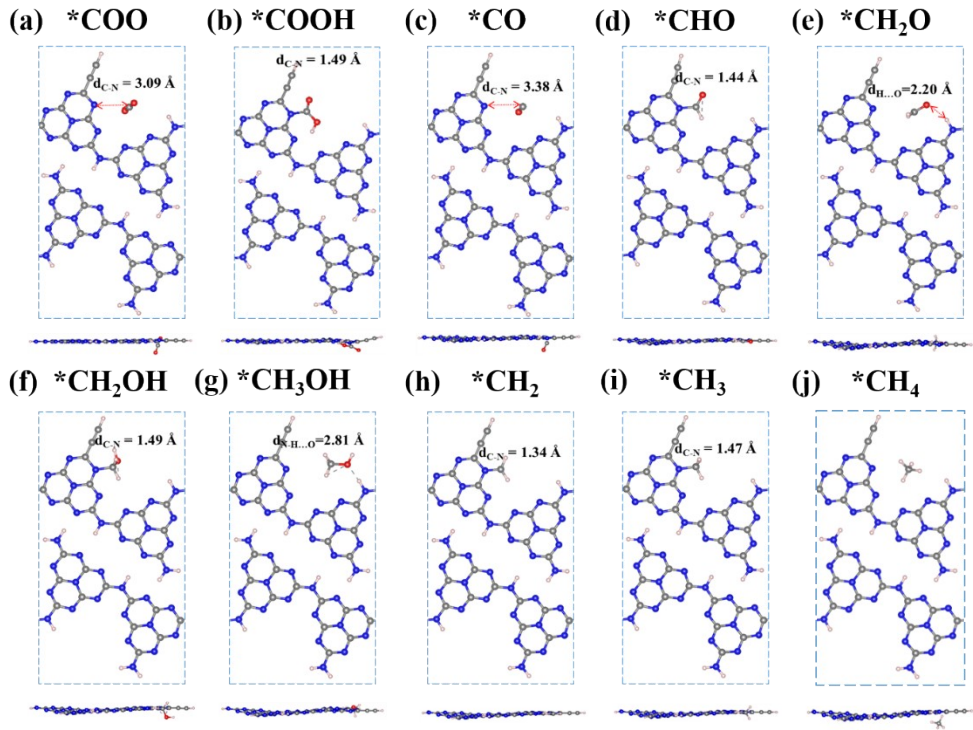


Fig. S11 Top and side views of the structure of the CO_2 reduction reaction intermediate of edge-modified melon-based CN nanoribbons (CCH-MNR), where grey, blue, pink, and red represent C, N, H, and O atoms.

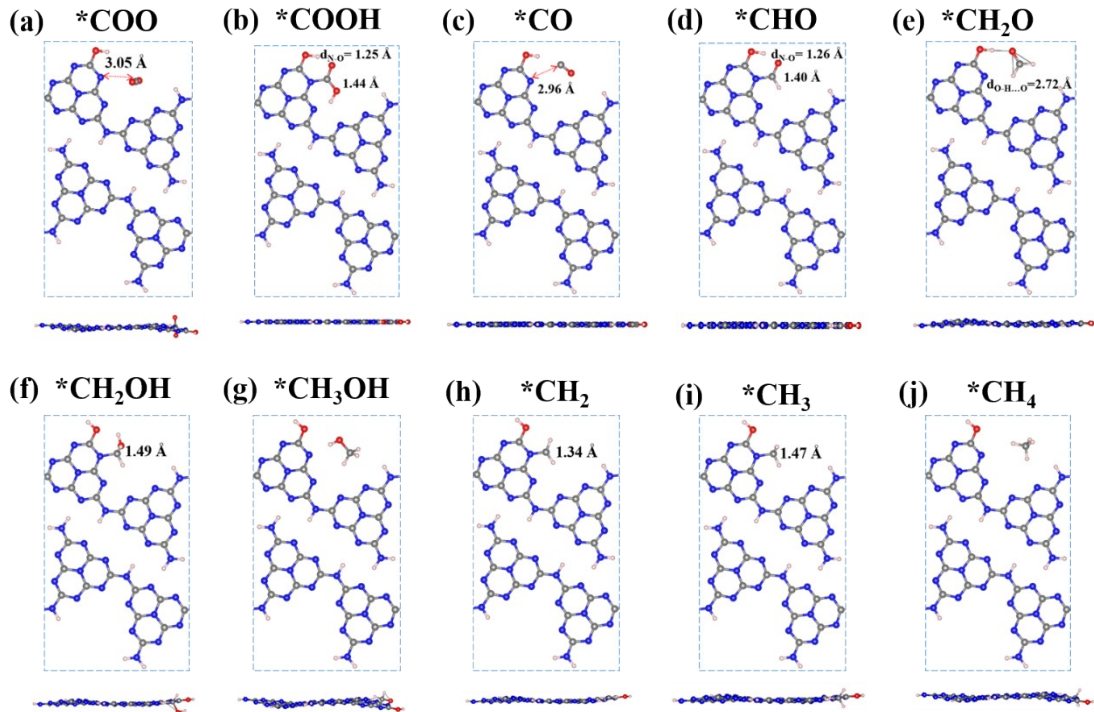


Fig. S12 Top and side views of the structure of the CO_2 reduction reaction intermediate of edge-modified melon-based CN nanoribbons (OH-MNR), where grey, blue, pink, and red represent C, N, H, and O atoms.

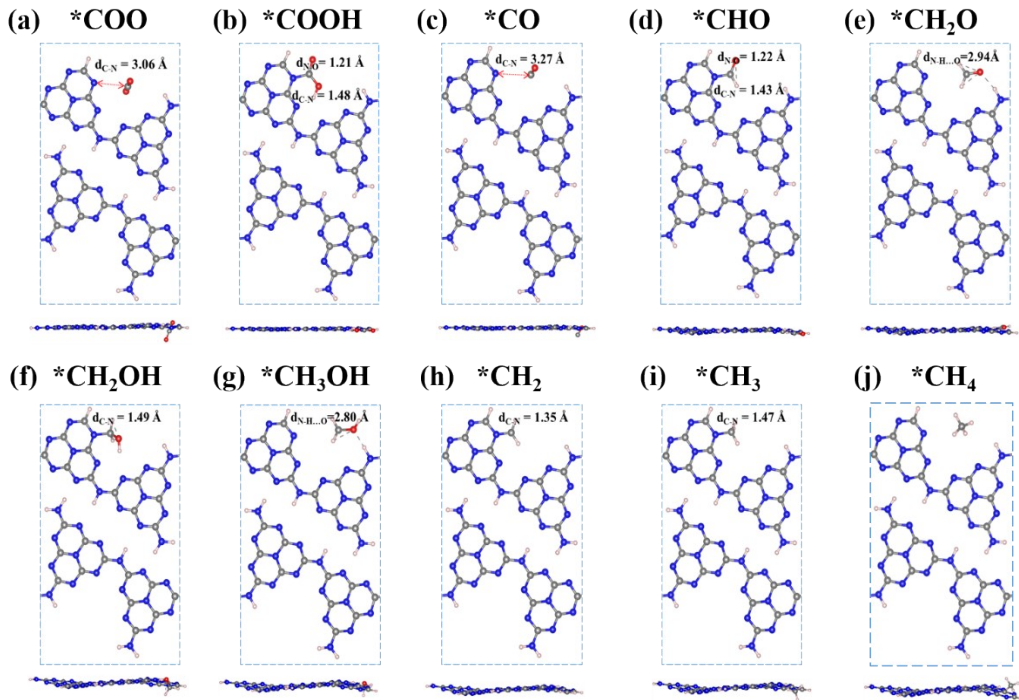


Fig. S13 Top and side views of the structure of the CO_2 reduction reaction intermediate of edge-modified melon-based CN nanoribbons (H-MNR), where grey, blue, pink, and red represent C, N, H, and O atoms.

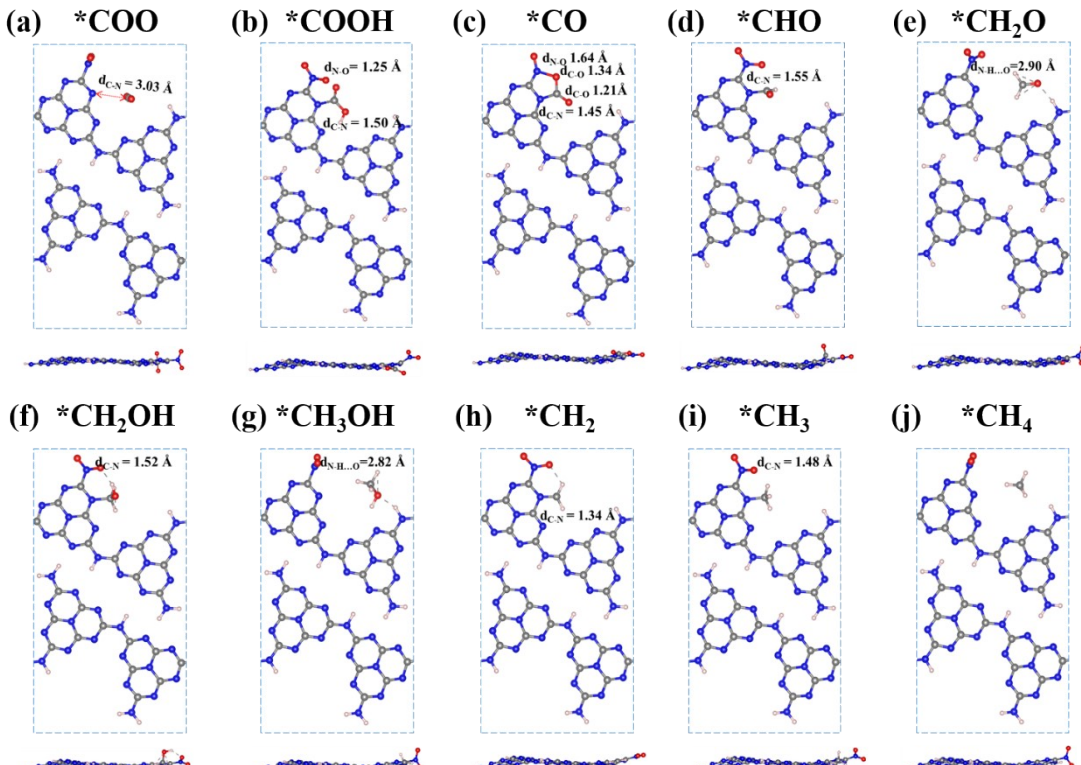


Fig. S14 Top and side views of the structure of the CO_2 reduction reaction intermediate of edge-modified melon-based CN nanoribbons (NO_2 -MNR), where grey, blue, pink, and red represent C, N, H, and O atoms.

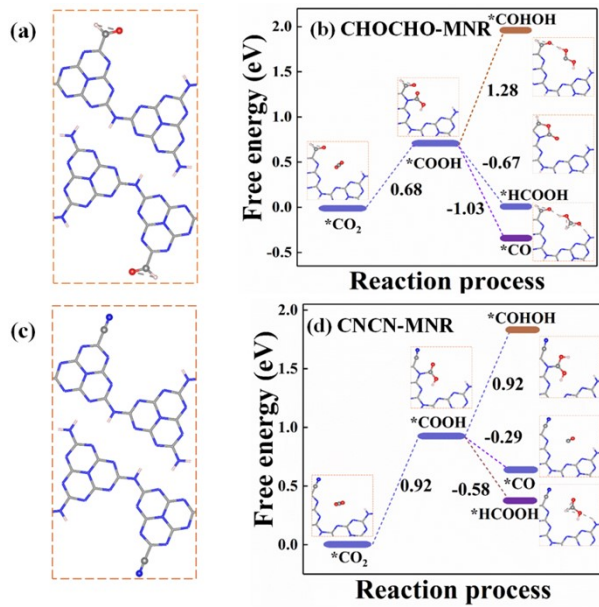


Fig. S15 The structure and two-electron reaction process of CO_2 reduction by CHOCHO-MNR (a and b) and by CNCN-MNR (c and d).

Table S1 Bader charge of -NH, Heptazine ring and functional group of edge-modified melon-based CN nanoribbons (X-MNRs, X = $-\text{NO}_2$, $-\text{CF}_3$, $-\text{CN}$, $-\text{CHO}$, $-\text{F}$, $-\text{Cl}$, $-\text{OH}$, $-\text{C}\equiv\text{CH}$, $-\text{SH}$, $-\text{CH}_3$, $-\text{H}$, $-\text{NH}_2$)

	Bader (-NH)	Bader (Heptazine ring)	Bader (Functional group)
$-\text{NO}_2$	-0.77	1.05	-0.35
$-\text{CF}_3$	-0.73	0.70	-0.05
$-\text{CN}$	-0.76	0.79	-0.16
$-\text{CHO}$	-0.68	0.56	0.07
$-\text{F}$	-0.65	1.23	-0.60
$-\text{Cl}$	-0.71	0.80	-0.15
$-\text{OH}$	-0.81	1.18	-0.45
$-\text{C}\equiv\text{CH}$	-0.67	0.64	-0.01
$-\text{SH}$	-0.71	0.50	0.19
$-\text{CH}_3$	-0.68	0.51	0.15
$-\text{H}$	-0.67	0.52	0.12
$-\text{NH}_2$	-0.68	1.05	-0.23

Table S2 Bader charge of C atoms (C1, C2, C3, C4, C5 and C6, labeled in Figure S1) of edge-modified melon-based CN nanoribbons (X-MNRs, X = -NO₂, -CF₃, -CN, -CHO, -F, -Cl, -OH, -C≡CH, -SH, -CH₃, -H, -NH₂)

	Bader (C1)	Bader (C2)	Bader (C3)	Bader (C4)	Bader (C5)	Bader (C6)
-NO ₂	1.57	1.57	1.54	1.61	1.48	1.42
-CF ₃	1.50	1.47	1.62	1.59	1.57	1.17
-CN	1.60	1.54	1.55	1.56	1.47	1.12
-CHO	1.50	1.57	1.55	1.51	1.50	1.04
-F	1.50	1.55	1.57	1.53	1.52	1.78
-Cl	1.48	1.51	1.61	1.52	1.56	1.32
-OH	1.60	1.59	1.55	1.61	1.47	1.60
-C≡CH	1.59	1.54	1.56	1.51	1.50	1.13
-SH	1.54	1.54	1.60	1.57	1.55	1.07
-CH ₃	1.52	1.52	1.59	1.53	1.48	1.15
-H	1.51	1.54	1.55	1.52	1.48	1.07
-NH ₂	1.50	1.57	1.54	1.61	1.54	1.50

Table S3 Bader charge of N atoms (N1, N2, N3, N4, N5, N6 and N7, labeled in Figure S1) of edge-modified melon-based CN nanoribbons (X-MNRs, X = -NO₂, -CF₃, -CN, -CHO, -F, -Cl, -OH, -C≡CH, -SH, -CH₃, -H, -NH₂)

	Bader (N1)	Bader (N2)	Bader (N3)	Bader (N4)	Bader (N5)	Bader (N6)	Bader (N7)
-NO ₂	-1.15	-1.15	-1.19	-1.14	-1.16	-1.16	-1.17
-CF ₃	-1.08	-1.10	-1.17	-1.22	-1.23	-1.21	-1.20
-CN	-1.12	-1.14	-1.19	-1.18	-1.16	-1.08	-1.18
-CHO	-1.12	-1.18	-1.21	-1.23	-1.15	-1.12	-1.12
-F	-1.13	-1.15	-1.21	-1.22	-1.17	-1.20	-1.14
-Cl	-1.10	-1.12	-1.20	-1.23	-1.16	-1.20	-1.21
-OH	-1.18	-1.15	-1.25	-1.18	-1.16	-1.13	-1.19
-C≡CH	-1.10	-1.14	-1.20	-1.22	-1.16	-1.12	-1.24
-SH	-1.19	-1.11	-1.22	-1.22	-1.23	-1.19	-1.21
-CH ₃	-1.18	-1.12	-1.24	-1.21	-1.10	-1.27	-1.15
-H	-1.13	-1.14	-1.21	-1.22	-1.17	-1.15	-1.13
-NH ₂	-1.12	-1.17	-1.20	-1.19	-1.16	-1.21	-1.16

Table S4 Total energy of CO₂ adsorption inside and outside the hole of melon-based CN nanoribbons

	<i>E</i> _{in}	<i>E</i> _{out}
<i>E</i> _{ads} (eV)	-0.31	-0.16

Table S5 The CO₂ adsorption energy, Bader charge of COOH, functional group and pyridine N atom on heptazine ring, and rate-determining Gibbs free energy difference of edge-modified melon-based CN nanoribbons (X-MNRs)

	$E_{\text{ads}}(\text{eV})$	Bader (COOH)	Bader (functional group)	Bader (Pyridine N)	$\Delta G (*\text{COO} \rightarrow *\text{COOH})$
-NO ₂	-0.232	0.385	-0.628	-1.15	0.99
-CF ₃	-0.275	0.354	-0.037	-1.08	1.17
-CN	-0.295	0.358	-0.088	-1.12	0.94
-CHO	-0.302	0.389	-0.025	-1.11	0.66
-F	-0.270	0.363	-0.593	-1.12	1.49
-Cl	-0.257	0.352	-0.109	-1.10	1.32
-OH	-0.32	0.329	-0.453	-1.18	1.17
-C≡CH	-0.288	0.394	0.017	-1.10	0.89
-SH	-0.275	0.345	0.239	-1.18	1.27
-CH ₃	-0.311	0.338	0.193	-1.18	1.11
-H	-0.28	0.325	0.215	-1.13	0.83
-NH ₂	-0.31	0.339	-0.235	-1.12	1.30

Table S6 Gibbs free energy of elementary reaction of melon-based CN and edge-modified melon-based CN nanoribbons (X-MNRs, X = -NH₂, -NO₂, -CN, -CHO, -C≡CH, -OH, -H)

	$\Delta G(*\text{HCOOH} \rightarrow *\text{ + HCOOH})$	$\Delta G(*\text{HCOOH} + \text{H}^+ \rightarrow *\text{CHO} + \text{H}_2\text{O})$	$\Delta G(*\text{CO} \rightarrow *\text{ + CO})$
Melon	0.72	1.41	-0.28
NH ₂ -MNR	0.98	1.55	-0.22
NO ₂ -MNR	0.65	0.92	0.61
CN-MNR	0.81	1.04	-0.28
CHO-MNR	0.88	1.12	0.77
CCH-MNR	0.92	1.18	-0.30
OH-MNR	0.89	1.30	-0.20
H-MNR	0.93	1.15	-0.33